Capacity of grillage foundations under horizontal loading

Knappett, Jonathan; Brown, Michael; Bransby, M. F.; Hudacsek, P.; Morgan, N.; Cathie, D.; Maconochie, A.; Yun, G.; Ripley, A. G.; Brown, N.; Egborge, R.

Published in:
Géotechnique

DOI:
10.1680/geot.12.OG.012

Publication date:
2012

Document Version
Publisher's PDF, also known as Version of record

Knappett, J. A. *et al.* (2012). *Géotechnique* **62**, No. 9, 811–823 [http://dx.doi.org/10.1680/geot.12.OG.012]

Capacity of grillage foundations under horizontal loading

J. A. KNAPPETT*, M. J. BROWN*, M. F. BRANSBY†, P. HUDACSEK*, N. MORGAN‡, D. CATHIE§, A. MACONOCHIE**, G. YUN**, A. G. RIPLEY††, N. BROWN‡‡ and R. EGBORGE††

Grillage foundations are an alternative to solid surface mudmats for supporting seabed infrastructure, offering improved hydrodynamic performance and savings in foundation material. Recent research has demonstrated that grillages can be designed to have similar vertical bearing capacity to a mudmat with the same footprint. This is extended herein by: (a) determining grillage performance under horizontal loading at constant vertical load (V-H); (b) the application and development of existing plasticity-based models for predicting performance; (c) comparing the V-H behaviour with surface mudmats; and (d) discussing the implications for design. Experimental tests were conducted in sands over a range of densities and in two different modes, representing different installation procedures. In over-penetrated tests, the foundations were installed to achieve a vertical bearing capacity V_0, followed by horizontal loading at a constant vertical load with $V < V_0$. In normally penetrated tests, foundations were installed to V_0 before horizontal loading at constant vertical load with $V = V_0$. Both normalised V-H yield surfaces and a plasticity-based simulation model are presented for use in design. Laboratory-scale grillages offer improved horizontal capacity in loose and medium-dense sands and similar horizontal capacity in very dense sand, compared with surface mudmats.

KEYWORDS: footings/foundations; model tests; offshore engineering; plasticity; sands

Les fondations à grillage constituent une solution alternative aux radiers pleins pour sols boueux destinés à supporter des infrastructures sur des fonds marins, renforçant les propriétés hydrodynamiques et réduisant la quantité de matières de fondations. Des travaux de recherche récents ont démontré qu'il est possible de concevoir des grillages présentant une portance verticale similaire sur un radier pour sols boueux de superficie égale. Pour ceci, cette communication présente (*i*) la détermination des performances du grillage sous l'effet de charges horizontales à charge verticale constante (*V-H*) ; (*ii*) l'application et le développement de modèles existants à base de plasticité pour la prédiction des performances ; (*iii*) la comparaison du comportement *V-H* avec les radiers pour sols boueux ; et (*iv*) des discussions sur les implications pour l'étude. Des essais expérimentaux ont été effectués sur des sables, dans toute une plage de densités et avec deux modes différents, représentant différentes procédures d'installation. Dans le cadre d'essais à « surpénétration », les fondations ont été installées pour réaliser une portance verticale V_0 suivie de charges horizontales à charge verticale constante $V < V_0$. Dans des essais à « pénétration normale », les fondations ont été installées à V_0 avant des charges verticales constantes avec $V = V_0$. Pour cette étude, on présente à la fois des surfaces de charge *V-H* normalisées et un modèle de simulation à base de plasticité pour des applications dans l'étude. Des grillages à l'échelle de laboratoire offrent une capacité horizontale renforcée dans des sables meubles et moyennement denses, et une capacité horizontale similaire dans des sables très denses, par rapport aux radiers pleins pour sols boueux.

INTRODUCTION

Grillage foundations represent an alternative to mudmats for installing infrastructure on the seabed, offering improved hydrodynamic performance in the splash zone and thereby simplifying and shortening installation operations in rough seas. A grillage consists of a series of thin vertical plates at close spacing, as shown in Fig. 1. Vertical loading of this foundation causes the plates to penetrate the seabed. If the plates are close enough, enhanced horizontal stresses can be generated in the soil between the plates, similar to the effect that leads to plugging in pipe piles (Randolph *et al.*, 1991). This leads to enhanced vertical capacity, and it is possible for the grillage to mobilise a bearing capacity similar to that of a solid mudmat with an equivalent-sized footprint, albeit at the expense of increased penetration. Bransby *et al.* (2012) derived a simple closed-form relationship for the bearing pressure of a grillage foundation in drained cohesionless soil and its relationship to vertical penetration as

$$z = \frac{1}{a} \ln \left[1 + \frac{aq(s/t)}{\gamma' N_{qB}} \right] \quad (1)$$

where q is the bearing pressure/capacity, z is the penetration of the grilles into the seabed, s is the grille spacing, t is the thickness of the individual grilles, γ' is the effective unit weight of the soil, N_{qB} is a bearing capacity factor related to the tips of the grilles taken from Berezantzev *et al.* (1961), and

$$a = \frac{2K \tan \delta'}{s - t} \quad (2)$$

where K is a coefficient of lateral earth pressure ($K \approx 1{\cdot}5K_0$, similar to displacement piles after Kulhawy, 1984), and δ' is the soil/grille interface angle of shearing resistance.

A subsequent programme of experimental testing was conducted at the University of Dundee to validate this solution, as part of a joint industry project between Acergy

Manuscript received 2 November 2011; revised manuscript accepted 9 May 2012.
Discussion on this paper closes on 1 February 2013, for further details see p. ii.
* University of Dundee, Dundee, UK.
† Advanced Geomechanics, Australia (formerly University of Dundee, UK).
‡ Lloyd's Register, Aberdeen, UK (formerly Cathie Associates, Brussels, Belgium).
§ Cathie Associates, Brussels, Belgium.
** Technip, Aberdeen, UK.
†† Subsea7, Aberdeen, UK.
‡‡ Subsea7, Norway.

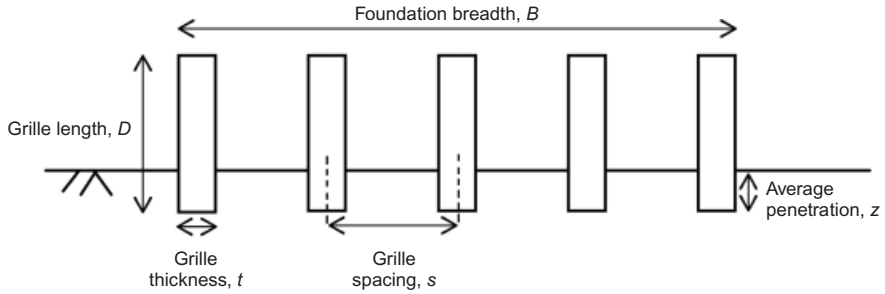

Fig. 1. Grillage geometry (not to scale)

(now Subsea 7), Subsea 7, Technip, Cathie Associates and the University of Dundee. Two main streams of testing were carried out under laboratory conditions: Series V, carried out to determine vertical capacity, V_0; and Series H, to find the vertical-horizontal (V-H) yield envelope. In both test series, grillages were tested with a reduced number of full-size grilles to reduce unwanted grain size or stress-level scaling effects. Tests were conducted in siliceous sand over a range of relative densities. The data from Series V are reported in Bransby *et al.* (2011), where they were used to validate and improve upon the aforementioned analytical solution. It was demonstrated that, in denser soils, dilation can lead to significant heave of the soil between the grilles, which had not been accounted for in the initial analytical solution. It was ultimately shown that the penetration (z_0) required to achieve the vertical capacity of a solid mudmat of the same overall footprint is given by

$$z_0 = \frac{\ln\left\{1 + K\tan\delta\left[B/(s-t)\right](s/t)\left(N_\gamma/N_{\mathrm{qB}}\right)(V/V_0)\right\}}{2K\tan\delta} \times (s-t) \quad (3)$$

where N_γ is the self-weight bearing capacity factor after Hansen (1970). Whereas the previous work was suitable for analysing the installation phase of a grillage foundation, describing the force required to install the foundation to provide the required vertical capacity or give a certain factor of safety against pure vertical loading (V_0/V), when foundations are in operation they will be subject to combinations of vertical, horizontal, moment and torsional loads. Grillage foundations are likely to be used for relatively light seabed infrastructure, including manifolds, pipeline end terminations (PLET) and temporary anchors. In most of these applications, horizontal load (H) will be applied relatively close to the level of the seabed (because these structures are relatively flat compared with their breadth), so that moment loads (M) are small (Cathie *et al.*, 2008).

This paper will discuss the combined vertical–horizontal (V-H) capacity of grillage foundations. Existing plasticity-based models will be applied and developed to describe the yield surface of grillages in V-H load space. These will be validated using experimental data from Series H, enabling comparison to be made between the performance of grillages and that of conventional surface mudmats.

EXPERIMENTAL METHOD

Overview

The aim of the tests conducted within Series H was to capture the detailed soil–grille interaction, rather than to model a specific prototype, and so full-scale grilles were tested (as described in Bransby *et al.*, 2011). A full-scale grillage foundation would have many grilles (of the order of 100); it was not feasible to test this under laboratory conditions, and so grillages consisting of $N = 8$ plates were used in the experiments. Centrifuge modelling was not considered a viable technique for testing the grillages, as even at very modest scale factors (such as 1:10) the thickness of the model grilles would be very close to the mean grain size of the soil, resulting in grain-size effects that would significantly affect the plugging behaviour between the grilles (e.g. for $t = 5$ mm in the prototype, at a scale of 1:10 this becomes 0·5 mm in the model, and d_{50} for the sand is 0·18, giving $t/d_{50} = 2{\cdot}8$). The implications of testing full-scale grille plates with reduced N on the extrapolation of the model test results to full scale will be discussed later. The grille plates were constructed from multiple smooth steel plates each of thickness $t = 5$ mm, length $L = 300$ mm (to give plane-strain conditions), and total height, including the region where the plates are fixed together, of $D = 150$ mm. They were connected together with bars and spacer blocks to ensure rigidity, and to ensure that each grille was parallel, and additionally allowing the spacing s between the grilles to be varied between tests.

Dry beds of uniformly graded fine silica sand ($d_{50} = 0{\cdot}18$ mm, $d_{10} = 0{\cdot}12$ mm, $\gamma'_{\max} = 17{\cdot}27$ kN/m^3 and $\gamma'_{\min} = 14{\cdot}33$ kg/m^3) were prepared at three different relative densities ($D_{\mathrm{r}} = 9\%$, 41% and 93%) in a clear-sided soil container 400 mm deep and 1 m wide, as shown diagrammatically in Fig. 2. The preparation methods used to prepare these samples are described in Bransby *et al.* (2011). A series of direct shear tests was performed on soil/soil and soil/steel interfaces, as also described in Bransby *et al.* (2011); the results are summarised in Table 1. These tests were undertaken at normal effective stresses of 10, 20 50, 100 and 200 kPa, to ensure that the failure envelopes applied equally well in the low- and high-stress ranges.

Test procedures

The model grillages were installed under vertical loading into clean fine silica sand, following an adaptation of the method used for the vertical load tests outlined in Bransby *et al.* (2011). Two types of Series H loading test were conducted: (a) *over-penetrated tests*; and (b) *normally penetrated tests*. Over-penetrated tests allowed for direct identification of V-H yield envelopes (described later), and would represent the installation of the foundation to achieve a certain capacity (V_0) by adding additional ballast (pre-loading), which is subsequently removed so that the foundation is loaded by a lower vertical load during operation ($V < V_0$), minimising subsequent service-state penetration. The normally penetrated tests reflect the case where the foundation is placed gently onto the seabed (with its superstructure already attached) and allowed to settle under its own weight.

In the over-penetrated tests, the foundation was first loaded

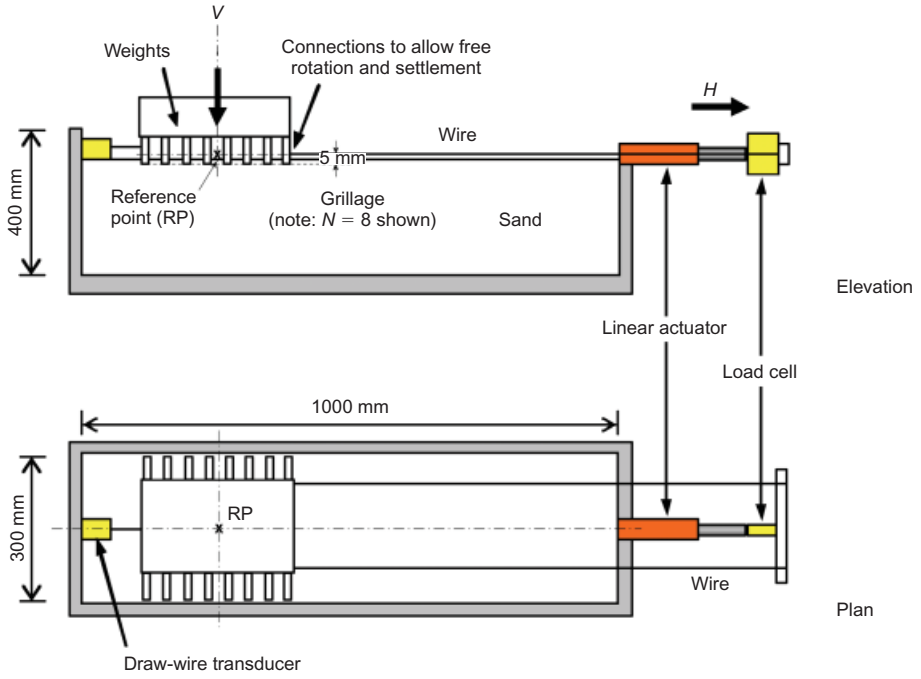

Fig. 2. Schematic diagram of grillage testing apparatus

Table 1. Soil properties

Soil density	ρ: kg/m^3	D_r: %	ϕ' (soil–soil): degrees	δ' (soil–grille): degrees
Loose	1487	9	30·8	21·7
Medium	1583	41	38·5	23·8
Dense	1739	93	42·3	24·9

vertically with dead weights (with subsequent resulting penetration z). These were placed on top of the grillage, with the centre of mass 200 mm above the reference point (RP) shown in Fig. 2. Then some of this vertical dead weight was removed, so that the foundation was unloaded vertically. Next, increasing horizontal displacement was applied through a long-stroke (300 mm) hydraulic actuator (see Fig. 2), which was connected to the foundation by way of a pair of wires, and moved at a rate of 0·4 mm/s under displacement control. The connection point was 5 mm above the bottom of the grilles (as close as practically possible), to approximate the $M = 0$ condition. The load and displacement reference point is shown in Fig. 2. A 10 kN capacity in-line tension–compression load cell was used to measure the resistance to the horizontal pull, and a draw-wire transducer was used to measure the horizontal movement of the foundation. Two linear variable differential transducers (LVDTs) (stroke length 50 mm; not shown) were also attached to the foundation 250 mm apart, pointing vertically upwards and reacting against a stationary horizontal beam. These two instruments allowed for the measurement of settlement and rotation of the foundation. In all tests there was initially at least 500 mm between the edge of the grillage and the wall of the container, to avoid any boundary effects.

In the normally penetrated tests, the foundation was placed carefully on the soil surface and then deadweight vertical load was applied. As this occurred, the penetration of the grillage foundation increased in line with the vertical load–penetration found from the vertical load tests (Series V). Once the target vertical load was achieved, this load was left on the foundation. The horizontal load was then applied in the same way as for the over-penetrated tests. The foundation in this case is described as normally penetrated because it is experiencing its maximum vertical loading when horizontal load is applied. The test arrangement is shown in Fig. 2.

The idealised behaviour of the two types of installation in V-H space are compared in Fig. 3. Fig. 3(a) shows the over-penetrated case, where the initial size of the yield surface is defined by V_0. On loading horizontally, the majority of the horizontal capacity is mobilised at very low lateral displacement (Fig. 4), and a clearly defined yield point is shown, at which the load path meets the initial yield envelope (at $H = H_y$). The plastic strain vector may also be approximated from the measurements of horizontal and vertical movements at the failure point, indicating the direction of motion of the foundation at yield. Beyond this point, the foundation response will work-harden as shown, until the foundation finds a steady-state depth (i.e. vertical displacement ceases) and the movement will become purely horizontal (at point Z in Fig. 3(a)). This is the *parallel point*, and is associated with the ultimate horizontal capacity of the foundation, as shown in Fig. 4 (point Z). The yield capacity (defined by H_y) would represent a conservative maximum horizontal load for use in design. Interpretation of the normally penetrated tests is more complicated. The foundation is initially installed to a given amount of penetration, such that $V = V_0$ (point A in Fig. 3(b)). Without unloading, the horizontal pull is then conducted. This causes the failure envelope to expand as the soil immediately starts yielding, with each increment in horizontal load causing the yield surface to expand (defined by V_{0B}, V_{0C} and V_{0D} in Fig. 3(b)). During this process, the foundation continues to embed itself as it is pulled laterally, by ever decreasing amounts (Fig. 4), as defined by the plastic strain vector, until the steady state is reached at the parallel point. If an over-penetrated and normally penetrated foundation were installed in the same soil, the same ultimate failure envelope would be reached (i.e. points Z and D would be at the same point in V-H load space). Tables 2 and 3 provide details of the grillage geometries and soil conditions used during testing.

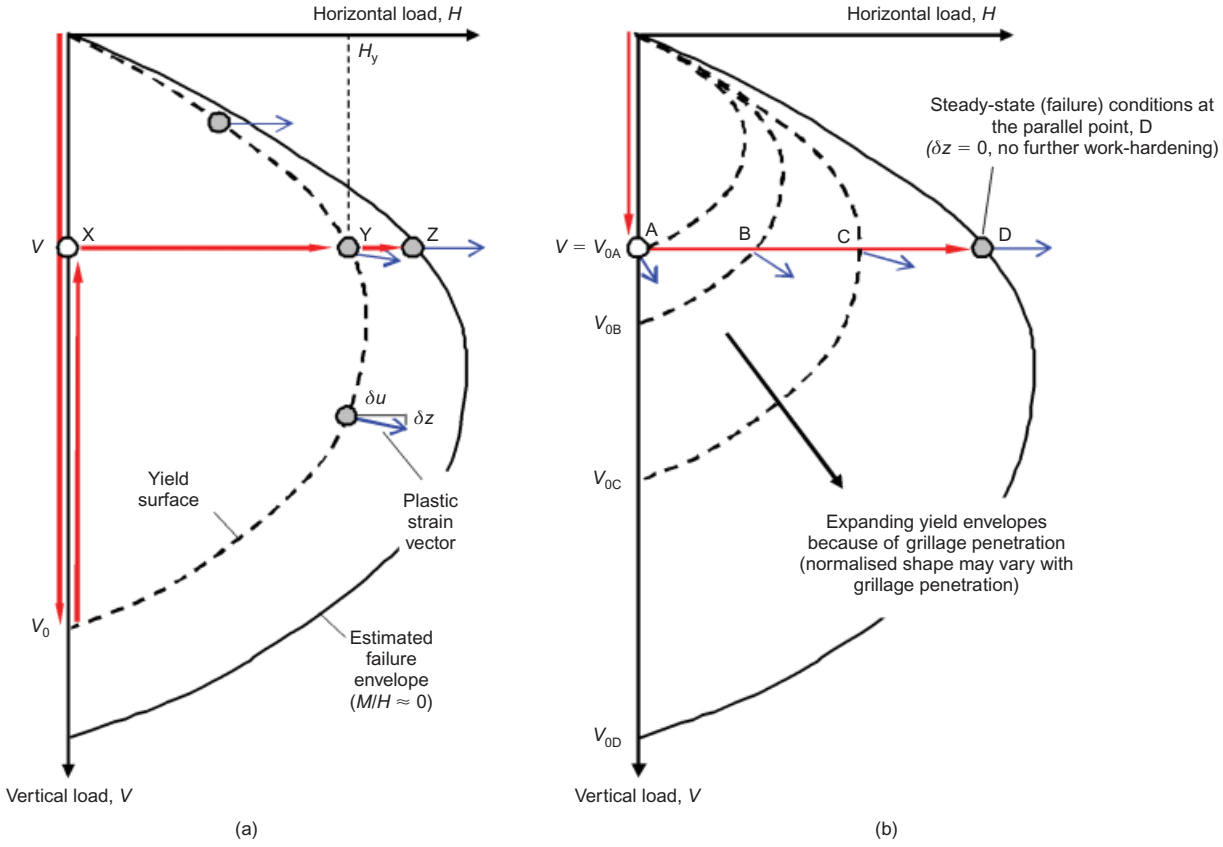

Fig. 3. Comparison of idealised V-H failure envelopes for grillage foundations: (a) over-penetrated case; (b) normally penetrated case

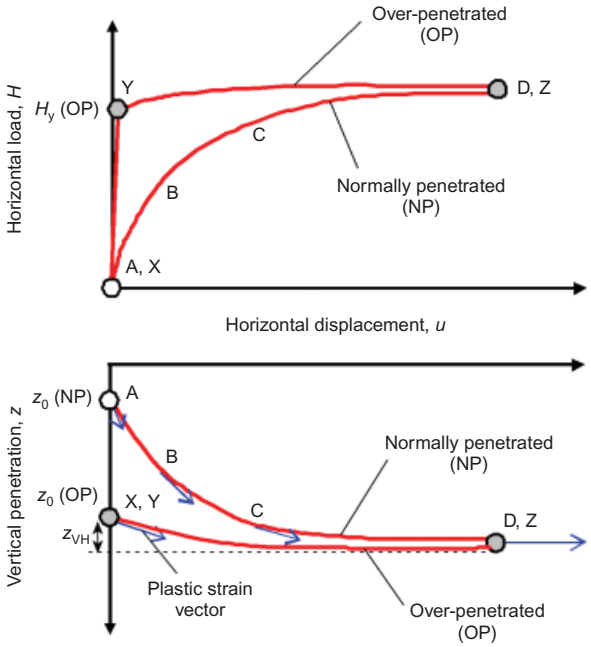

Fig. 4. Idealised load–deformation behaviour

RESULTS

Figure 5 shows the horizontal force–displacement behaviour and footing trajectory for an over-penetrated and normally penetrated test at the same vertical load V. The initial yield point (Y, $H = H_y$) is immediately evident for the over-penetrated test with very small 'elastic' displacements (both vertical and horizontal), and the load path (XY) is within the initial yield surface (i.e. $H < H_y$). The normally penetrated foundation shows significant work-hardening (additional penetration) to reach a capacity similar to that of the over-penetrated foundation, which is associated with greatly increased vertical penetration during horizontal loading (z_{VH}, as defined in Fig. 4). Comparing Figs 4(a) and 5(a), it is also clear that in both cases the observed load–displacement response continues to work-harden after the initial yield, despite the foundation trajectory becoming horizontal. Visual observations demonstrated that this was due to the formation of a berm in front of the displacing grillage.

Over-penetrated grillages

The yield envelope for a surface-bearing solid mudmat on sand under general V-H-M loading was approximated by Nova & Montrasio (1991) and Martin (1994). For pure V-H loading, as considered herein, this has an approximately parabolic shape, given by

$$\frac{H}{V_0} = h_0 \beta \left(\frac{V}{V_0} + \chi\right)^{\beta_1} \left(1 - \frac{V}{V_0}\right)^{\beta_2} \tag{4}$$

where

$$\beta = \frac{(\beta_1 + \beta_2)^{(\beta_1+\beta_2)}}{\beta_1^{\beta_1} \beta_2^{\beta_2} (1+\chi)^{(\beta_1+\beta_2)}} \tag{5}$$

In equations (4) and (5), V represents the vertical load applied to the foundation from the superstructure, plus the weight of the foundation itself. The term h_0 in equation (4) represents the maximum horizontal capacity normalised by the maximum vertical capacity. The parameters β, β_1 and β_2 are yield surface shaping parameters, and it is conventionally assumed that $\beta_1 \approx \beta_2 \approx 1$. The value of the non-dimensional

Table 2. Testing programme: over-penetrated tests

Test ID	s/t	Density	Preload V_0, dead load V: N	z_0: mm	H_y: N	$\delta z^p/\delta u^p$	B: mm
H7	4	Loose	753, 162	37·1	133	0·243	145
H8	4	Loose	753, 330	41·1	175	0·417	145
H9	4	Loose	753, 497	36·2	140	0·935	145
H10	4	Loose	1503, 330	52·8	240	0·106	145
H11	4	Loose	1503, 647	59·8	340	0·212	145
H12	4	Loose	1503, 993	45·5	305	0·379	145
H16	4	Medium	753, 162	17·0	92	0·379	145
H17	4	Medium	753, 330	16·4	110	0·493	145
H18	4	Medium	753, 497	18·3	120	0·607	145
H22	4	Dense	753, 162	11·2	67	0·417	145
H23	4	Dense	753, 330	12·1	83	0·554	145
H24	4	Dense	753, 497	12·4	107	0·622	145
H28	8	Loose	756, 182	54·8	190	0·076	285
H29	8	Loose	756, 331	59·3	200	0·380	285
H30	8	Loose	756, 497	49·5	170	2·660	285

Table 3. Testing programme: normally penetrated tests

Test ID	s/t	Density	Preload V_0, dead load V: N	z_0: mm	H ($u = 50$ mm): N	z_{VH} ($u = 50$ mm): mm	B: mm
H5	4	Loose	162, 162	13·9	150	26·0	145
H6	4	Loose	330, 330	19·4	352	40·6	145
H13	4	Medium	162, 162	4·9	99	15·8	145
H14	4	Medium	330, 330	7·8	200	22·9	145
H15	4	Medium	497, 497	14·6	237	25·9	145
H19	4	Dense	162, 162	3·7	103	11·7	145
H20	4	Dense	330, 330	5·6	190	17·5	145
H21	4	Dense	497, 497	5·8	242	24·3	145
H25	8	Loose	182, 182	20·8	245	27·9	285
H26	8	Loose	331, 331	33·4	349	28·4	285
H27	8	Loose	497, 497	48·9	492	17·1	285
H31	8	Dense	182, 182	4·1	133	20·0	285
H32	8	Dense	330·6, 330·6	8·5	221	26·0	285
H33	8	Dense	497·3, 497·3	14·9	390	33·0	285

parameter χ can be solved when $V = 0$, and relates to the initial horizontal capacity of the foundation H_0. For $\beta_1 = \beta_2 = 1$

$$\frac{\chi}{(1+\chi)^2} = \frac{H_0}{4h_0V_0} \tag{6}$$

For an over-penetrated grillage that penetrates the soil by z, prior to the application of the in-service V-H loading, three effects will contribute to H_0. First, as the interface between the soil and the foundation is predominantly soil/soil (as $s > t$), the interface friction angle will be (approximately) ϕ', rather than an interface value δ'. Second, in a widely spaced grillage, the weight of the trapped soil between the grilles ($V_{tr} = \gamma' BLz$) will enhance the vertical effective stress at the soil/foundation interface, acting in addition to V. Note, however, that a solid mudmat of equivalent footprint may have a higher footing weight than the grillage, which may counteract the benefit from the trapped soil. Third, the embedment of the grilles will generate additional net passive resistance (H_p) acting on the outside of the foundation of

$$H_p = 0{\cdot}5(K_p - K_a)\gamma' z^2 L \tag{7}$$

where K_p and K_a are the passive and active earth pressure coefficients respectively. This term will be significant for the model grillages, but is likely to be less significant in larger foundations (with high N). Therefore

$$H_0 = V_{tr}\tan\phi' + H_p \tag{8}$$

In equations (4) and (6), V_0 will be known for the grillage (this is the load that was applied to over-penetrate the grillage during installation), and H_p can be determined using equation (7), where z represents the initial penetration of the seabed at V_0. The initial seabed penetration z may be calculated using equation (3) from Bransby *et al.* (2012) in dense sand, and using z^* in loose and medium sand to account for heave of the soil between the grilles, following the recommendations of Bransby *et al.* (2011), where

$$z^* = z\left(1 + \frac{1}{s/t - 1}\right) \tag{9}$$

Figure 6 shows test data for over-penetrated grillages with $s/t = 4$ in loose sand for grillages penetrated to two different initial vertical capacities, V_0. Also shown in this figure are yield surfaces of the form of equation (4) plotted both for the grillages (fitting the experimental data using a least-squares procedure) and for a solid surface mudmat of equivalent footprint. For the surface footings $h_0 = 0{\cdot}125$, as suggested by Butterfield & Gottardi (1994) and Byrne & Houlsby (2001), among others. For the grillages, values of $h_0 = 0{\cdot}23$ and $0{\cdot}22$ were obtained by the data-fitting procedure for the tests at 753 N and 1503 N respectively. The

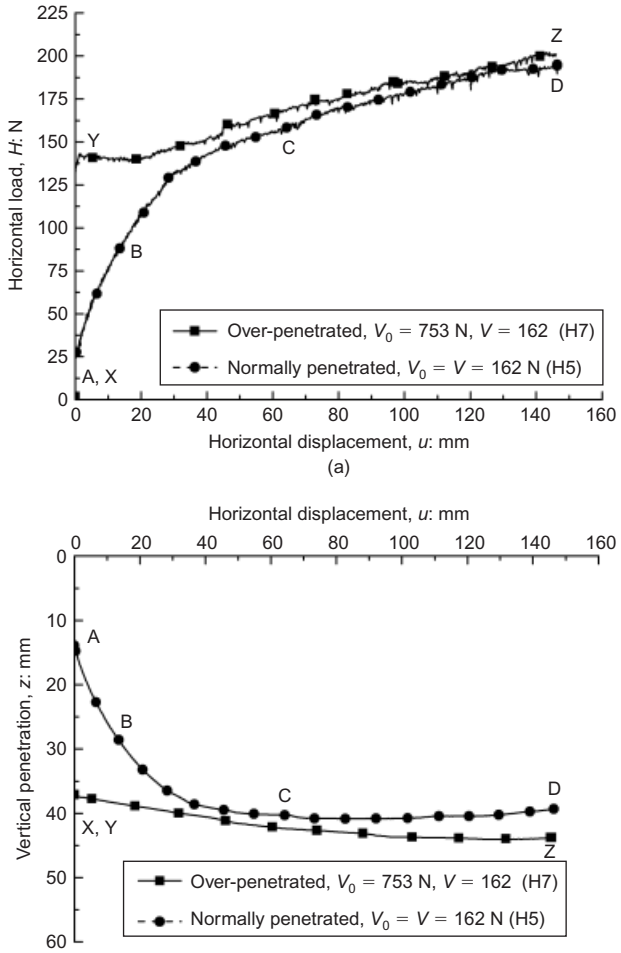

Fig. 5. Comparison of measured horizontal force–displacement behaviour for over-penetrated and normally penetrated tests at same vertical load V: (a) horizontal force–displacement behaviour; (b) footing trajectory

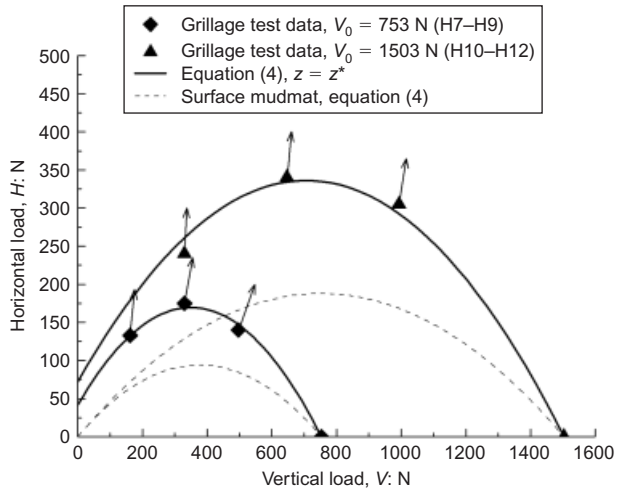

Fig. 6. Calculated V-H failure envelopes (equation (4)) for over-penetrated grillages compared with typical surface mudmats ($s/t = 4$, loose sand)

yield surfaces for the grillages are fitted to a much smaller number of data points than those previously derived for surface mudmats. Furthermore, in a full-scale grillage foundation, H_p will be negligibly small compared with $V_{tr} \tan \phi'$ (equation (8)), such that H_0 would approach that of a full-scale mudmat.

For the two sets of test data in loose sand, the shape of the yield surface can be explained entirely by the change in H_0 due to the different initial penetrations in the $V_0 = 753$ N and $V_0 = 1503$ N tests, with h_0 being independent of V_0. Also shown in Fig. 6 are yield surfaces for a surface mudmat (i.e. zero penetration) having a vertical capacity V_0, plotted using equation (4). The plotted mudmat solution does not account for the effects of embedment (as reported for sands by e.g. Byrne & Houlsby, 2001; Butterfield, 2006; Govoni *et al.*, 2011), a small amount of which will occur because of elastic settlement under applied vertical load. Further tests were conducted on stiff steel strip footings, 85 mm wide, placed on the loose and dense sands, which demonstrated settlements of $z_0 = 3{\cdot}4$ mm and $2{\cdot}1$ mm at an applied load of V_0. Based on Butterfield (2006), this would result in only a small expansion of the yield surface (in the H/V_0 direction) of 8% and 4% respectively (the grillages in the loose sand case are larger by approximately $0{\cdot}22/0{\cdot}125 = 176\%$).

Figure 7 shows normalised yield surfaces for over-penetrated tests with $s/t = 4$. Both H and V are normalised by V_0, as this is defined directly by the installation process. Data are shown for the three different densities of sand that were tested. It can be seen that, as the density increases, the shape of the yield surface changes, which is represented by a reduced value of h_0 in equation (4). The values of h_0 for the medium-dense and dense soils are $0{\cdot}15$ and $0{\cdot}12$ respectively. The test data points for $V/V_0 > 0{\cdot}5$ in the medium and dense sands do not appear to fit the earlier trends, and these data points were not included in the fit. The predicted position of the yield surface would, however, give a conservative estimate of capacity. $V/V_0 < 0{\cdot}5$ is a more likely in-service condition, so that the foundation has some margin of safety against vertical bearing failure. A comparative normalised yield surface for a solid mudmat is also shown in Fig. 7. These results demonstrate that grillages in loose and medium-dense soils are likely to outperform surface mudmats under V-H loading. In dense soil, their performance is likely to be similar to that of a surface mudmat. This demonstrates that over-penetrated grillage foundations may be a more attractive foundation design in poor-quality soils, where their perceived weakness of sacrificing vertical penetration to achieve sufficient vertical capacity becomes a strength under in-service V-H loading. Fig. 8 shows the effect of s/t ratio on V-H performance in loose sand. For the same V_0, the yield surface for the more widely spaced

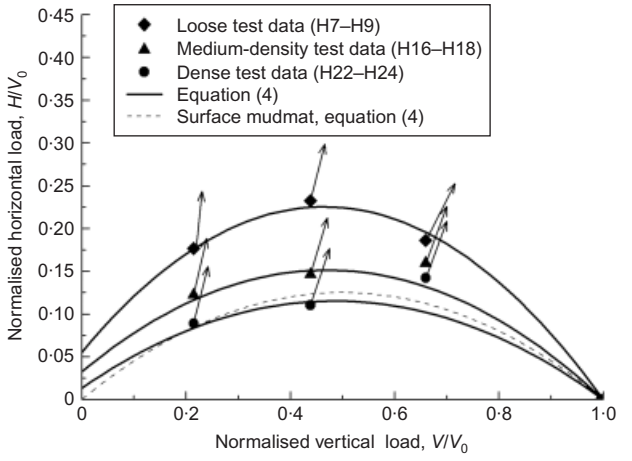

Fig. 7. Comparison of normalised yield surfaces for over-penetrated grillage tests at different densities with yield surfaces for surface mudmats ($s/t = 4$, $V_0 = 753$ N)

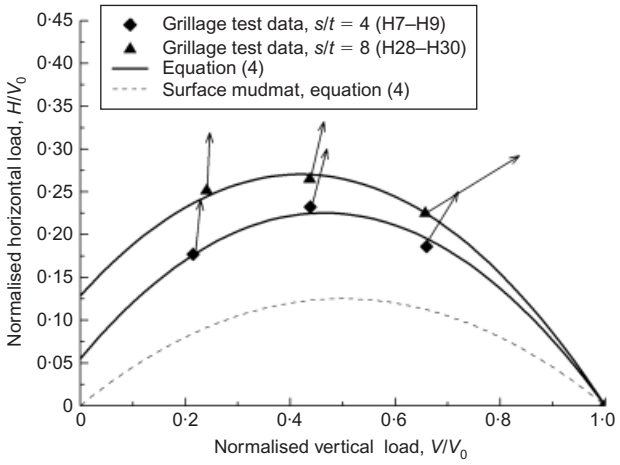

Fig. 8. Comparison of normalised yield surfaces for over-penetrated grillage tests at different s/t with yield surfaces for surface mudmats ($V_0 = 753$ N, loose sand)

grillage is larger ($h_0 = 0{\cdot}27$), as the foundation is penetrated more deeply to achieve the same V_0 (cf. equation (3)).

To put these results into the context of other common shallow foundations used offshore, Fig. 9 shows values of h_0 derived for surface mudmats, skirted and embedded circular foundations (reported in Villalobos *et al.*, 2009), and for the grillages reported in this study. The data are plotted against a normalised embedment parameter. For the grillages, this is the initial penetration normalised by the foundation width (z_0/B); for the skirted foundations this is the embedded length of the skirt (l) normalised by the foundation diameter ($2R$). Fig. 9 implies that any increase in foundation capacity of a grillage over that of a surface mudmat occurs primarily from increased embedment, in a similar way to a skirted foundation. The data in Fig. 9 should not, however, be used to infer directly that a grillage will necessarily perform better than a skirted footing, as the reference points are not the same in each case. In all of the foregoing discussion, the $M = 0$ condition is only approximated in the tests, and any rotation of the grillage would cause additional moments due to second-order effects as the vertical load is displaced horizontally above the reference point. As the shape of the yield surface will vary in the H–M plane (not investigated in this study), this would be likely to reduce the values of the fitting parameter h_0 determined in the H–V plane.

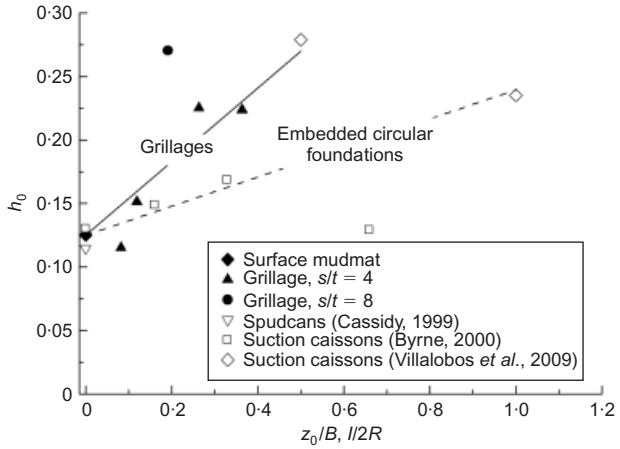

Fig. 9. Comparison of non-dimensional horizontal capacity between grillages and other typical offshore foundations

Normally penetrated tests

In the normally penetrated tests, plastic yielding starts immediately on application of H, the foundation continually displacing and expanding the yield surface until the parallel point is reached. In such a case, the yield surface alone is insufficient for defining the horizontal capacity, as this will be strongly dependent on the magnitude of the plastic strains, and these strains may themselves provide additional constraints on the design. Therefore a more advanced model that accounts for plastic flow is required for such a case, and will be developed in this section. The much larger horizontal and vertical displacements that occur in these tests (see Fig. 5) mean that a significant amount of soil will be displaced into a passive wedge in front of the translating model grillage, which will result in the formation of a sizeable berm above the soil surface, increasing H_p and therefore H_0 above the value given by equations (7) and (8) respectively. If, before an increment of horizontal displacement, the grillage is initially penetrated by z_i into the seabed, the swept volume of soil (δV_{swept}) that is moved by the grillage due to foundation displacements δu and δz in the horizontal and vertical directions respectively is approximated by

$$\delta V_{\text{swept},i+1} = \left(z_i \delta u + \frac{\delta u \delta z}{2}\right) L \tag{10}$$

as shown in Fig. 10. Berm formation will occur from passive failure within the soil ahead of the displacing grillage, so consideration of the geometry of a passive wedge of soil (formed by a slip plane at an angle $\theta = 45 - \phi'/2$ to the horizontal, as shown in Fig. 10) will suggest the extent of the affected soil ahead of the foundation. From Fig. 10, the width of the berm ahead of the foundation (w_s) will then be

$$w_{s,i+1} = (z_i + \delta z) \tan\left(45 - \frac{\varphi'}{2}\right) \tag{11}$$

The volume of the soil in the berm is described by

$$V_{\text{berm},i+1} = \xi w_{s,i+1} h_{s,i+1} L \tag{12}$$

where h_s is the height of the berm adjacent to the grillage, and ξ is a numerical factor accounting for the shape of the berm. If $\xi = 1$ the berm is rectangular, whereas if $\xi = 0{\cdot}5$ the berm will be triangular. Assuming that δV_{swept} is significantly larger than any elastic compression of the soil, then $\Sigma \delta V_{\text{swept}}$ must be equal to the volume of soil within the berm, from which $h_{s,i+1}$ can be found

$$h_{s,i+1} = \frac{\sum_{i=1}^{i+1} \delta V_{\text{swept}}}{\xi (z_i + \delta z) \tan[45 - (\phi'/2)]} \tag{13}$$

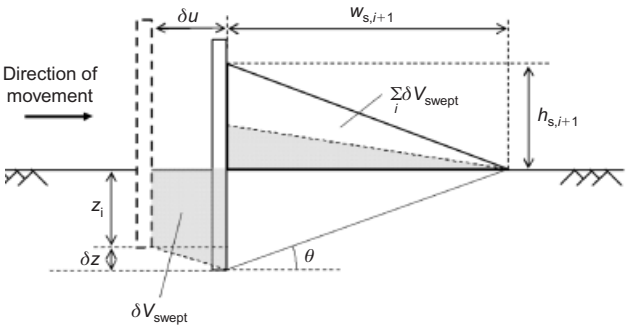

Fig. 10. Idealised berm formation during lateral deformation of a penetrated grillage

The berm will apply a surcharge at the surface of the seabed of $\xi\gamma' h_{s,i+1}$, so that H_p becomes

$$H_{p,i+1} = 0{\cdot}5(K_p - K_a)\gamma'(z_i + \xi h_{s,i+1})^2 L \quad (14)$$

This replaces equation (7) for a normally penetrated grillage. If the berm does not form before the horizontal capacity is reached (as for the over-penetrated tests), then $h_{s,i+1} = 0$, and equation (14) reduces to equation (7). Additionally, the berm cannot increase in height indefinitely, owing to the finite height of the grilles (D). Therefore, if the sum of the penetration below the soil surface ($z_i + \delta z$) and the berm height above the soil surface ($h_{s,i+1}$) is greater than D, the height of the berm will be limited to

$$h_{s,i+1}|_{max} = D - (z_i + \delta z) \quad (15)$$

Equations (10)–(15) can incrementally account for the formation of the berm, requiring only basic and derived soil properties (ϕ', γ', K_p, K_a), geometric properties (ξ) and a set of compatible incremental displacements (δu, δz). These last two quantities are related to each other by the flow rule, which is derived from the potential function $g(V, H)$, as described for other shallow foundation problems by Nova & Montrasio (1991), Martin (1994) and Houlsby & Cassidy (2002). A summary of previous modelling of the flow rule in sands is given in Houlsby (2003). Assuming that the shape of the yield surface throughout the normal penetration process is given by equation (4), the yield function $f(V, H)$ may be written as

$$f(V, H) = \frac{4h_0}{(1+\chi)^2}\left(\frac{V}{V_0} + \chi\right)\left(1 - \frac{V}{V_0}\right) - \frac{H}{V_0} = 0 \quad (16)$$

for the case $\beta_1 = \beta_2 = 1$. Based on the observed directions of the plastic potentials in the over-penetrated tests (Figs 6–8) a potential function was proposed, described by

$$g(V, H) = \zeta\left(\frac{V}{V_0}\right)^2 + \left(\frac{H}{V_0}\right)^2 - 1 = 0 \quad (17)$$

The hardening rule (based on the increasing penetration of the grillage) is defined by equation (1).

The underlying function in equation (17) is that of a simple circular arc, although this is compressed in the V/V_0 direction by the parameter ζ. This *associativity parameter* reduces the magnitude of the vertical plastic displacements compared with those in the horizontal direction, an approach that has previously been adopted for shallow foundations by Martin (1994). A value of $\zeta = 0{\cdot}15$ was found to give a good match over the full normally penetrated dataset. The gradient of the plastic potential ($\delta z^p/\delta u^p$) is then given by

$$\frac{\delta z^p}{\delta u^p} = \frac{\partial g}{\partial V}\left(\frac{\partial g}{\partial H}\right)^{-1} \quad (18)$$

giving

$$\frac{\delta z^p}{\delta u^p} = \frac{\zeta(1+\chi)^2(V/V_0)}{4h_0[(V/V_0)+\chi][1-(V/V_0)]} \quad (19)$$

The load–penetration curve for a normally penetrated grillage may be found numerically, following the flow chart in Fig. 11. In this algorithm, the initial pass through the flow chart sets the initial conditions of the grillage following installation, namely $V = V_0$, $z = z_0$ (see Bransby *et al.*, 2011, 2012), $u = H = 0$. Following this, the grillage penetration is increased by δz after horizontal loading, and the increased capacity V_0 (due to the work-hardening) is calculated. As V is constant (representing the superstructural load), $V/V_0 < 1$,

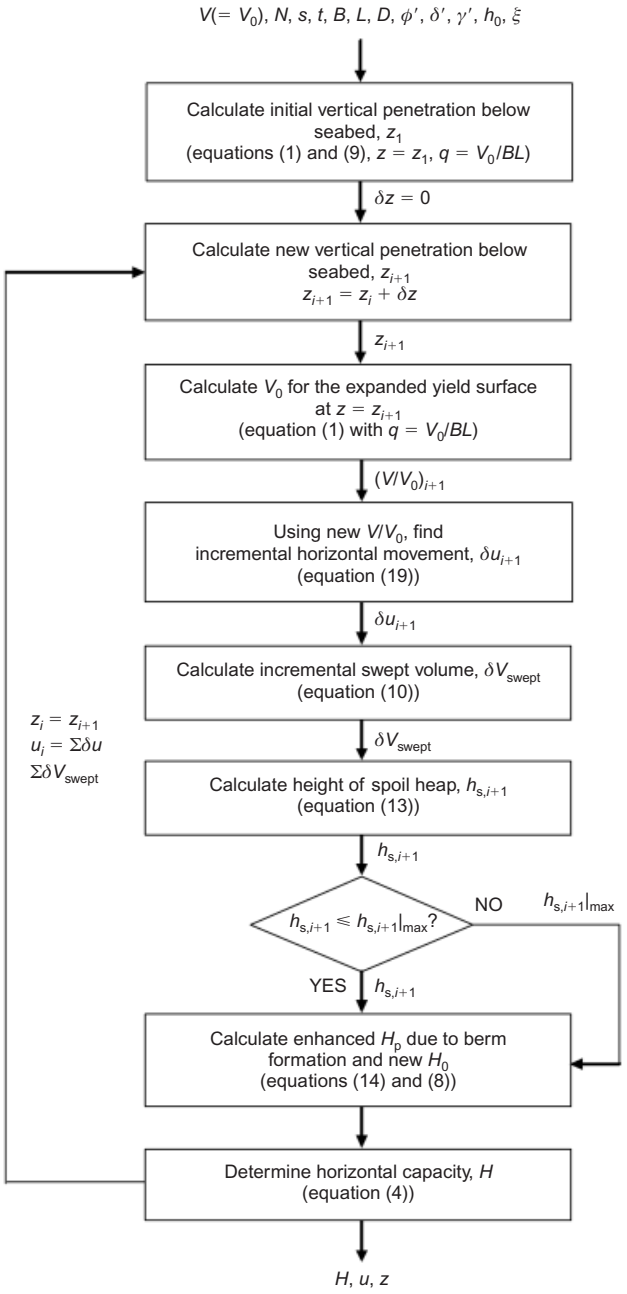

Fig. 11. Flow chart for simulating load–deformation behaviour of a grillage foundation using plasticity model developed herein

and the grillage loading condition has moved onto a new expanded yield surface. The horizontal displacement δu is calculated from the plastic potential, allowing berm formation and hence H_0 at that increment to be determined. As a normally penetrated foundation is always yielding plastically, the horizontal force associated with the displacement of the grillage (δu^p, δz^p) can then be found using equation (4) with the new V/V_0 and H_0. From Fig. 11, the input data required consist of the geometrical properties of the grillage (N, s, t, B, L, D), soil properties (ϕ', δ', γ') and model parameters (h_0, ξ). Simulations have been performed for all of the normally penetrated tests detailed in Table 3, using the soil properties given in Table 1, assuming $\xi = 0{\cdot}5$ (i.e. the berm is triangular in shape) and using $\delta z^p = 1$ mm between increments. The values of h_0 determined from the over-penetrated tests were used (for dense sand at $s/t = 8$, $h_0 = 0{\cdot}12$ was assumed). Extension of this model to consider any rotation of the footing would be a non-trivial extension of the method proposed above, requiring the yield surface

and plastic potential function in the H–M plane (data for which were not collected as part of this study).

Figures 12–14 show comparisons of model predictions (simulations) with measured model test data. Figs 12 and 13 show that the load–displacement (H–u) curves for grillages at closer spacing ($s/t = 4$) are generally well reproduced by the plasticity-based model described above, even to very large displacements and in soils of different density. The predictions of the footing trajectory (z–u), which are controlled by the flow rule, while reasonably close at smaller values of u, diverge during the latter stage of each test. This implies that there may be a better plastic potential function than the simple relationship assumed in equation (17) that is a closer fit to the true underlying behaviour. However, it is unlikely that such large lateral displacements would be tolerable under in-service conditions, and so the ability to model the behaviour accurately at large displacement is likely to be of limited practical use. Comparing Figs 13 and 14, it is apparent that the model performs less well for larger grille spacing. However, it is unlikely that such large s/t would be used in practice, as such a foundation would require excessive initial penetration during installation to support a significant vertical load (Bransby *et al.*, 2011).

Figure 15(a) shows the values of V/V_0 and H/V_0 throughout the simulations. Each simulation appears to sweep around a single normalised yield surface, owing to the assumption of self-similar yield surfaces during plastic yielding. The test data from the over-penetrated tests are also shown in this figure, to demonstrate that the yield surface

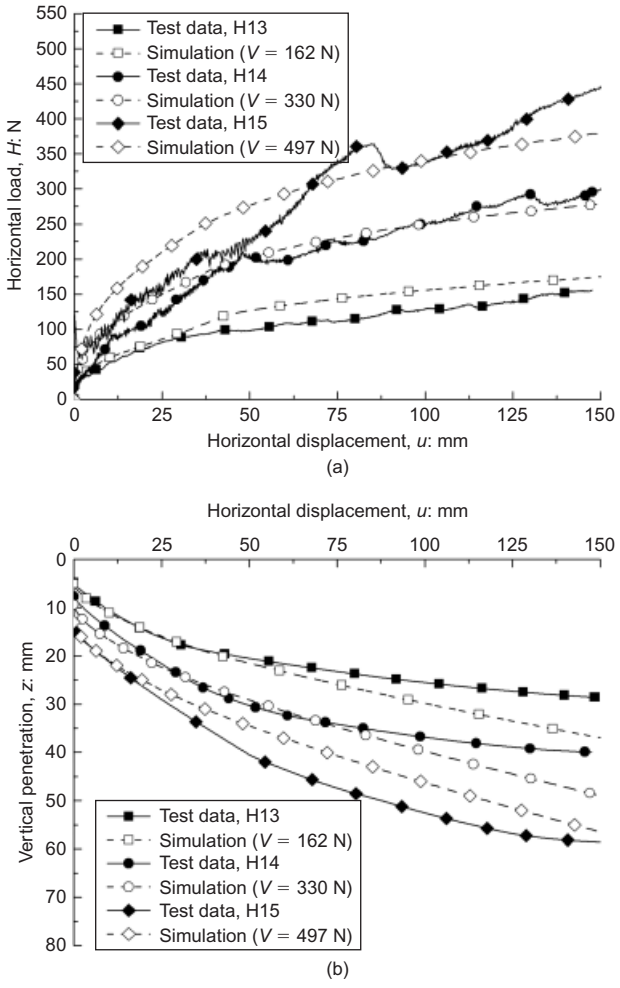

Fig. 12. Comparisons of simulations and test data for normally penetrated grillages in medium-dense sand ($s/t = 4$): (a) horizontal force displacement behaviour; (b) footing trajectory

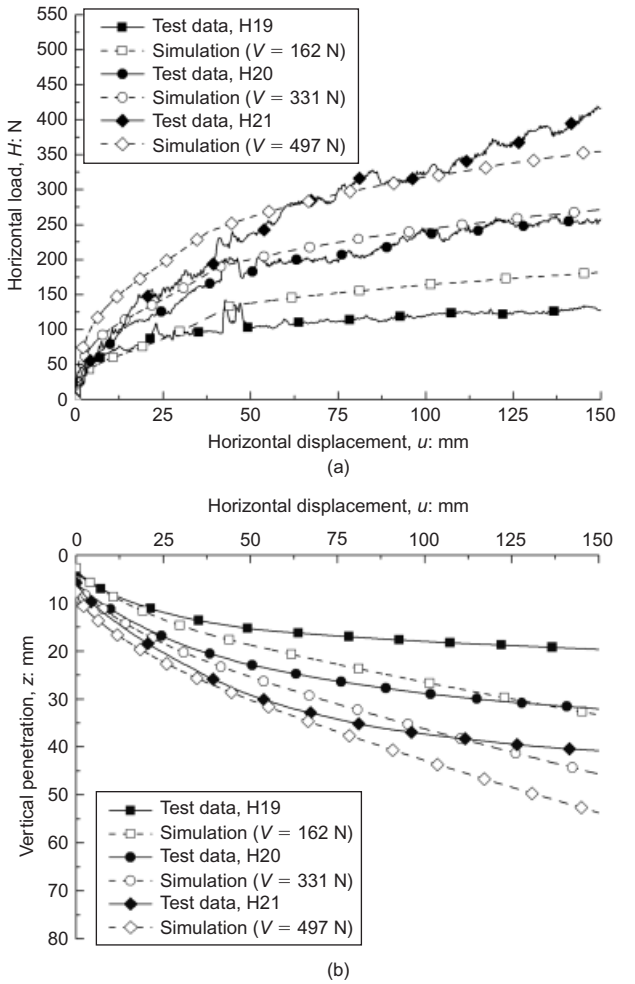

Fig. 13. Comparisons of simulations and test data for normally penetrated grillages in dense sand ($s/t = 4$): (a) horizontal force–displacement behaviour; (b) footing trajectory

assumptions used in the normally penetrated model match the yield surfaces derived from the over-penetrated grillages. There are some small variations in shape at lower values of V/V_0 due to the effect of the incremental berm formation, which was not present in the over-penetrated cases at $H = H_y$. Fig. 15(b) shows the computed plastic potential $\delta z/\delta u$ as a function of V/V_0 for the same simulations, compared with the plastic potentials observed at yield in the over-penetrated tests (assuming elastic displacements are comparatively small), which similarly show good agreement.

Taking $u = 50$ mm as a practical limit on tolerable foundation movement, Fig. 16 summarises the horizontal capacity at this displacement, normalised by the applied vertical load, for all of the normally penetrated test data. The model appears to underpredict capacity in the loose soil, based on the limited amount of data available, particularly for larger s/t, compared with the medium-dense and dense soil data from Figs 12–14, which are also summarised in Fig. 16. Also shown in this figure is the maximum value of H/V ($= \tan\delta'$) possible for a surface mudmat. It can be seen that in all cases the grillages are an acceptable replacement for a solid surface mudmat. These observations are consistent with those for the over-penetrated grillages presented previously.

Figure 17 summarises the penetration information for all of the normally penetrated model tests and simulations at $u = 50$ mm. Fig. 17(a) considers the initial penetration z_0 following installation. Data from the over-penetrated tests are also shown in this figure. This essentially provides further validation of the vertical load–penetration model

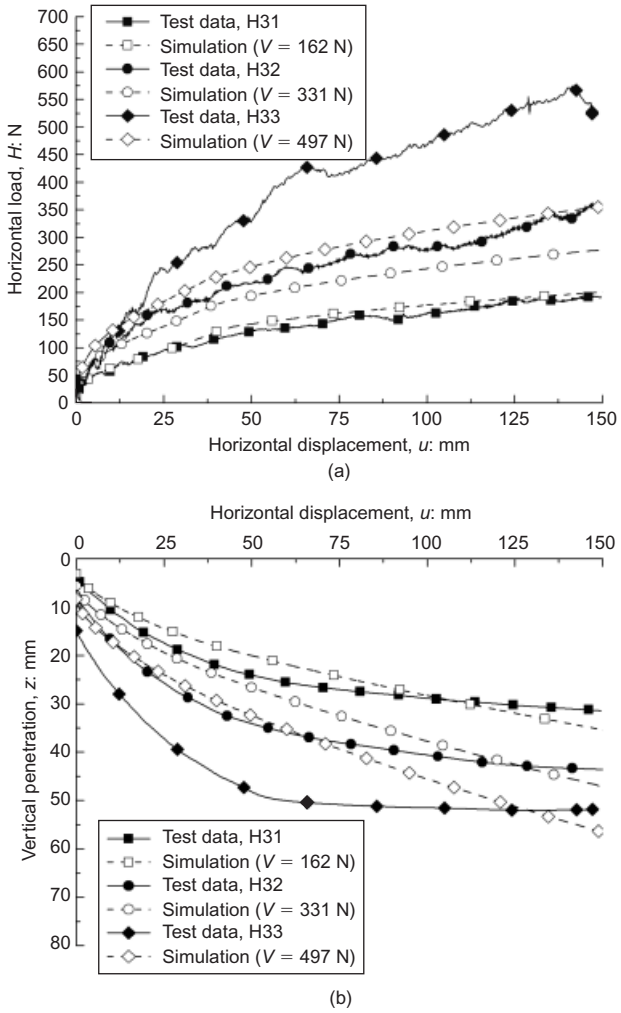

Fig. 14. Comparisons of simulations and test data for normally penetrated grillages in dense sand ($s/t = 8$): (a) horizontal force–displacement behaviour; (b) footing trajectory

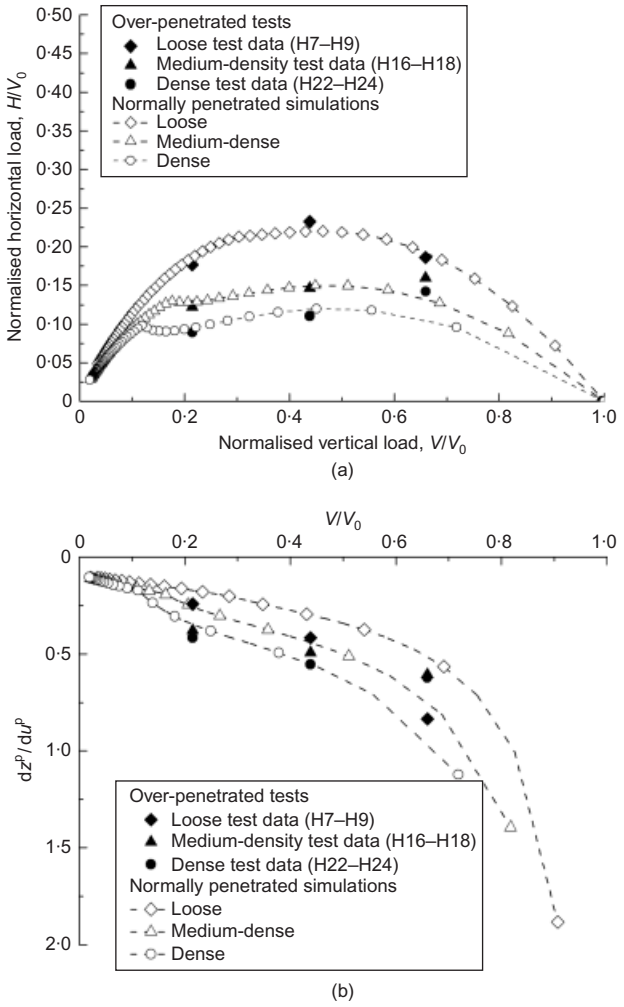

Fig. 15. Comparisons of normalised load–deformation behaviour from simulations with over-penetrated test data ($s/t = 4$): (a) yield surfaces; (b) plastic potentials

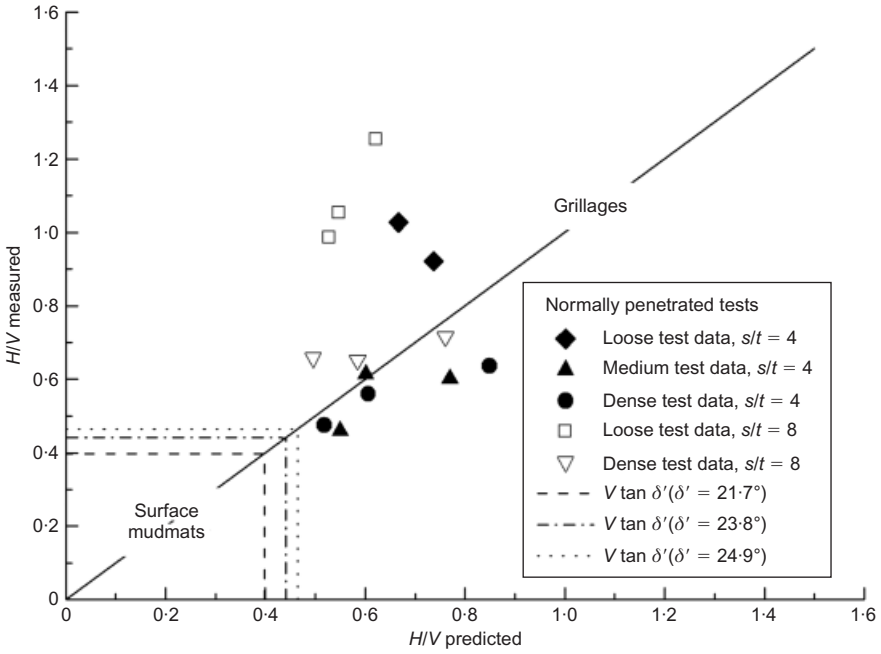

Fig. 16. Comparisons of normalised horizontal foundation capacity at $u = 50$ mm between simulations and measured test data

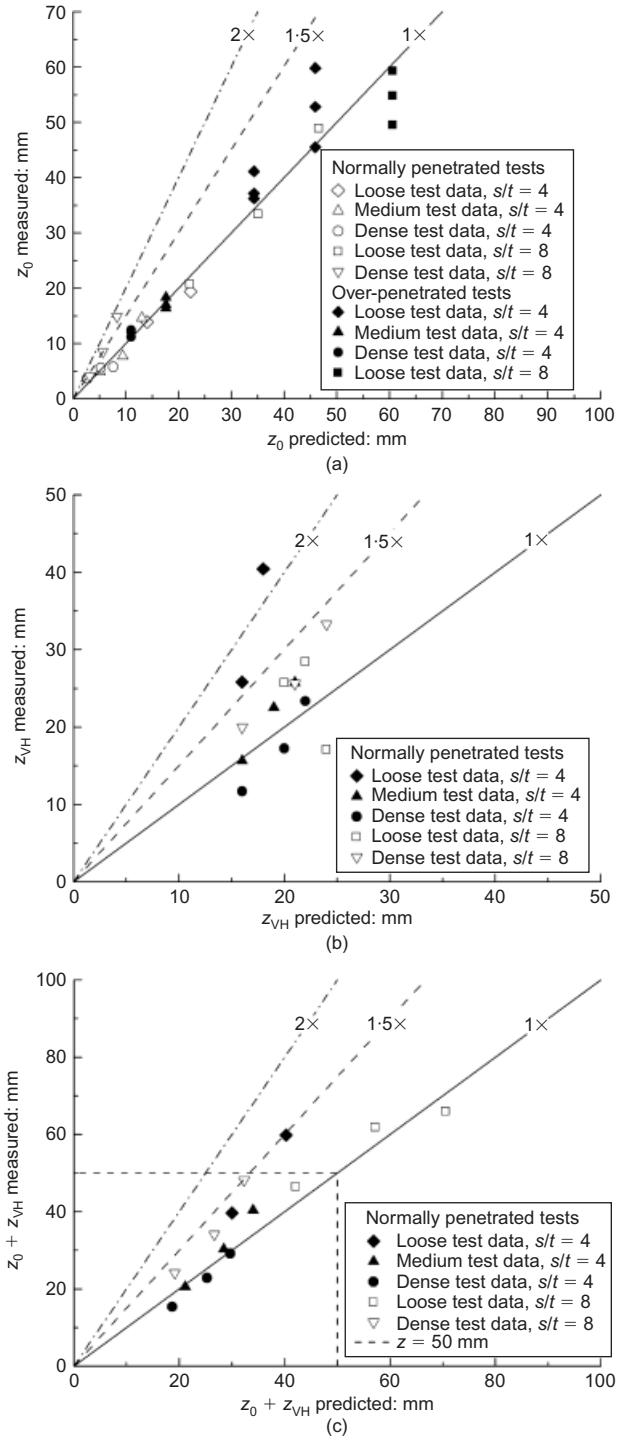

Fig. 17. Comparisons of vertical penetration of grillage foundations between simulations and measured test data: (a) initial penetration, z_0; (b) additional penetration due to V-H loading at $u = 50$ mm; (c) total penetration at $u = 50$ mm

(equation (1)) from Bransby *et al.* (2012) against an additional dataset (none of the Series H tests in Tables 2 or 3 was reported in the earlier publication). Fig. 17(b) shows the additional penetration occurring due to V-H loading to $u = 50$ mm (z_{VH}). The agreement between the simulations and the test data appear adequate for $s/t = 4$ (a more likely configuration than $s/t = 8$, owing to vertical considerations) in the medium-dense and dense sands. This figure also demonstrates that horizontal displacement of a normally penetrated grillage will result in significant additional settlement under combined in-service loading, the effects of which must additionally be considered in terms of the serviceability of the supported infrastructure. In comparison, the additional settlement of over-penetrated grillages is much smaller during this phase (cf. Fig. 5). Finally, Fig. 17(c) shows the combined penetrations following installation and in-service loading to $u = 50$ mm. Considering a limit on total settlement of $z = 50$ mm (a typical grille height for a grillage foundation; see Bransby *et al.*, 2012), it is clear that large values of s/t should be avoided in the design of grillages that will be installed in a normally penetrated mode.

The penetration values shown in Fig. 17 will not be representative of a wider full-scale grillage foundation with many more grilles. This is because the hardening law (equation (1)) is highly non-linear with N ($\approx B/s$), as demonstrated previously by Bransby *et al.* (2012). Fig. 18 shows how z is expected to scale as additional plates are added (without changing the ratio V/V_0) to make the foundation wider. For a 2 m wide foundation, for example, having $N = 100$ for $s/t = 4$ and $N = 50$ for $s/t = 8$, the initial penetration would be expected to be approximately twice the value observed in the model tests for $N = 8$ at $s/t = 4$, and approximately 60% greater for $s/t = 8$. Assuming that the plastic potential function is the same (i.e. $\delta u^p/\delta z^p$ does not change with increasing N), then the lateral displacements may be similarly increased as N is increased. This is accounted for analytically in the plasticity model described herein but, clearly, further full-scale testing is required to experimentally validate the model to large N.

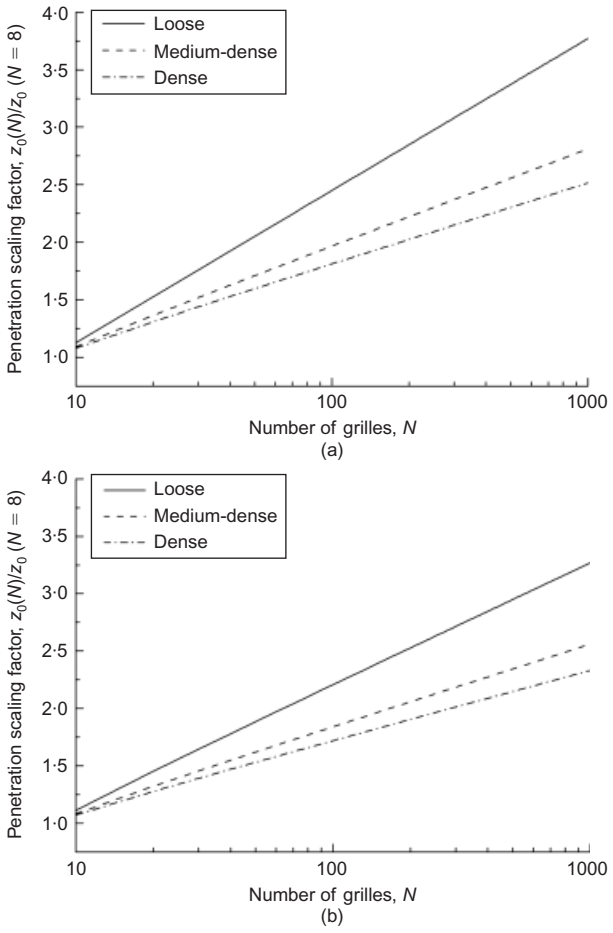

Fig. 18. Scaling of vertical penetration with increased N at different relative densities; (a) $s/t = 4$; (b) $s/t = 8$

CONCLUSIONS

This paper describes the behaviour of grillage foundations under horizontal loading at a constant vertical load in sand based on small-scale model tests, and applies and develops existing plasticity-based models for predicting capacity and deformation that have been validated against the model test database. The plasticity models are validated against only a relatively small database of small-scale (1g) model tests. Model grillage foundations in loose and medium-dense sand offer improved capacity under V-H (in-service) loading compared with equivalent solid surface mudmats with the same vertical bearing capacity. This additional capacity is chiefly provided by: (a) enhanced interface friction due to soil–soil rather than soil–foundation shearing; and (b) a yield surface that is expanded in the H/V_0 direction, owing to penetration of the grillage. In dense sand, the behaviour of a grillage is very similar to that of the surface of a mudmat (owing to reduced penetration). In the model tests presented herein, there was additionally passive resistance due to the penetration of the foundation, although this is likely to be negligibly small compared with (a) and (b) for a full-scale foundation. The plasticity-based model used herein predicts the horizontal capacity well in medium-dense and dense sands, and underpredicts slightly in loose sand. In all cases tested, the grillages have been shown to be an acceptable replacement for a solid mudmat under V-H loading.

The results of the model study suggest that if a prototype grillage is installed under its self-weight and that of the supported structure (normally penetrated), initial penetration during installation will be small, although significant displacement (both horizontal and vertical) of the foundation will occur under initial horizontal loading. In contrast, if the foundation is over-penetrated to $V_0 > V$, initial penetration will be larger, but a significant horizontal yield capacity can be mobilised with negligible additional penetration. In both cases the lateral foundation response will be strain-hardening due to the increasing vertical penetration. At large displacements, the two foundations will ultimately exhibit similar capacity and total penetration, although in the normally penetrated case most of the penetration will occur in service, whereas in the over-penetrated case most of the penetration will occur during installation. It may therefore be beneficial for grillages to be installed using additional ballast where possible (over-penetrated), as foundation movements will be more damaging in service (e.g. when connected as part of an operating field) than during installation. As this study is based upon laboratory testing with reduced grille numbers, further full-scale testing is required to validate the proposed analytical models for foundations with large numbers of grilles.

ACKNOWLEDGEMENTS

The experimental work was carried out as part of a joint industry project funded by Acergy (now Subsea7), Subsea 7 and Technip. The project was managed by Cathie Associates. The authors wish to thank their employers for permission to publish this paper. The views expressed are those of the authors alone, and do not necessarily represent the views of their respective companies.

NOTATION

a $2K \tan \delta'/(s - t)$
B foundation breadth
D grille length
D_r relative density
d_{10} particle size at which 10% of particles are smaller
d_{50} mean particle size
H horizontal load
H_0 horizontal sliding capacity at $V = 0$
H_y horizontal yield capacity of over-penetrated grillage foundation
H_p passive component of horizontal capacity
h_0 non-dimensional horizontal capacity
h_s berm height adjacent to foundation
K coefficient of lateral earth pressure
K_0 coefficient of lateral earth pressure at rest
K_a coefficient of lateral active earth pressure
K_p coefficient of lateral passive earth pressure
L foundation length
l embedment depth of a circular foundation
M moment
N number of grilles
N_γ, N_{qB} bearing capacity factors
q foundation bearing pressure
R radius of embedded circular foundation
s grille spacing
t grille thickness
u horizontal foundation displacement
δu^p increment of plastic horizontal displacement
V vertical load
V_0 vertical foundation capacity
V_{berm} volume of soil in berm
V_{tr} additional vertical load due to trapped soil between grilles
w_s width of berm ahead of displacing foundation
z vertical grille penetration
z^* vertical grille penetration including heave
z_{VH} additional vertical penetration due to V-H loading
z_0 vertical grille penetration to obtain equivalent mudmat capacity
δz^p increment of plastic vertical penetration
β, β_1, β_2 non-dimensional yield surface shaping parameters
γ' effective unit weight of soil
δ' angle of interface friction
ζ associativity parameter
θ angle of slip plane to the horizontal
ξ shape factor (berm)
ϕ' angle of internal friction of soil
χ apparent non-dimensional tension

REFERENCES

Berezantzev, V. G., Khristoforov, V. S. & Golubkov, V. N. (1961). Load bearing capacity and deformation of piled foundations. *Proc. 5th Int. Conf. Soil Mech. Found. Engng, Paris*, 11–15.

Bransby, M. F., Brown, M. J., Knappett, J. A., Hudacsek, P., Morgan, N., Cathie, D., Maconochie, A., Yun, G., Ripley, A. G., Brown, N. & Egborge, R. (2011). The vertical capacity of grillage foundations in sand. *Can. Geotech. J.* **48**, No. 8, 1246–1265.

Bransby, M. F., Knappett, J. A., Brown, M. J. & Hudacsek, P. (2012). The vertical capacity of grillage foundations. *Géotechnique* **62**, No. 3, 201–211, http://dx.doi.org/10.1680/geot.9.P.131.

Butterfield, R. (2006). On shallow pad-foundations for four-legged platforms. *Soils Found*. **46**, No. 4, 427–435.

Butterfield, R. & Gottardi, G. (1994). A complete three-dimensional failure envelope for shallow footings on sand. *Géotechnique* **44**, No. 1, 181–184, http://dx.doi.org/10.1680/geot.1994.44.1.181.

Byrne, B. W. (2000). *Investigations of suction caissons in dense sand*. DPhil thesis, University of Oxford, UK.

Byrne, B. W. & Houlsby, G. T. (2001). Observations of footing behaviour on loose carbonate sands. *Géotechnique* **51**, No. 5, 463–466, http://dx.doi.org/10.1680/geot.2001.51.5.463.

Cassidy, M. J. (1999). *Non-linear analysis of jack-up structures subject to random waves*. DPhil thesis, University of Oxford, UK.

Cathie, D. N., Morgan, N. & Jaek, C. (2008). Design of sliding foundations for subsea structures. *Proc. 2nd BGA Foundations Conf. (ICOF2008), Dundee*, 813–823.

Govoni, L., Gourvenec, S. & Gottardi, G. (2011). A centrifuge study on the effect of embedment on the drained response of shallow foundations under combined loading. *Géotechnique* **61**, No. 12, 1055–1068, http://dx.doi.org/10.1680/geot.7.00109.

Hansen, J. B. (1970). *A revised and extended formula for bearing capacity.* Bulletin No. 28, pp. 5–11. Copenhagen, Denmark: Danish Geotechnical Institute.

Houlsby, G. T. (2003). Modelling of shallow foundations for offshore structures. *Proc. 1st BGA Foundations Conf. (ICOF2003), Dundee*, 1–16.

Houlsby, G. T. & Cassidy, M. J. (2002). A plasticity model for the behaviour of footings on sand under combined loading. *Géotechnique* **52**, No. 2, 117–129, http://dx.doi.org/10.1680/geot.2002.52.2.117.

Kulhawy, F. H. (1984). Limiting tip and side resistance, fact or fallacy. *Proceedings of the symposium on analysis and design of piled foundations*, San Francisco, CA, pp. 80–98.

Martin, C. M. (1994). *Physical and numerical modelling of offshore foundations under combined loads*. DPhil thesis, University of Oxford, UK.

Nova, R. & Montrasio, L. (1991). Settlements of shallow foundations on sand. *Géotechnique* **41**, No. 2, 243–256, http://dx.doi.org/10.1680/geot.1991.41.2.243.

Randolph, M. F., Leong, E. C. & Houlsby, G. T. (1991). One dimensional analysis of soil plugs in pipe piles. *Géotechnique* **41**, No. 4, 587–598, http://dx.doi.org/10.1680/geot.1991.41.4.587.

Villalobos, F. A., Byrne, B. W. & Houlsby, G. T. (2009). An experimental study of the drained capacity of suction caisson foundations under monotonic loading for offshore applications. *Soils Found*. **49**, No. 3, 477–488.